Adaptive Filtering Methods for RSSI Signals in a Device-Free Human Detection and Tracking System

Apidet Booranawong, Nattha Jindapetch, *Member, IEEE*, and Hiroshi Saito, *Member, IEEE*

***Abstract*—In a device-free human detection and tracking system using a received signal strength indicator (RSSI), the change in the RSSI pattern is monitored and analyzed to detect and track the human movement. The variation in measured RSSI signals is one of the major effects leading to significant detection and tracking error. To handle such a research problem, in this paper, we propose adaptive RSSI filtering methods designed by considering both the detection and tracking accuracy and the computational complexity. The novelty of our proposed filtering methods is that, to reduce the computational complexity, the measured RSSI input values are automatically filtered only when they have high variation levels; an appropriate threshold is set and used for the decision. Additionally, to increase the detection and tracking accuracy, the measured RSSI input values with different variation levels are filtered with different filtering levels adaptively. The proposed filtering methods are verified by the experiments, which have been carried out in an indoor environment. Various human movement patterns with different directions and speeds are tested. The experimental results show that, with our test scenarios, the proposed filtering methods can appropriately reduce the RSSI variation. They provide good detection and tracking accuracy, which is measured by the number of times the system can detect and track the human with the correct zone. The computational complexity measured by the number of mathematical operations, used by the proposed methods, is lower than comparative filtering methods.**

***Index Terms*—Accuracy, adaptive filtering methods, complexity, device-free detection and tracking, human movements, RSSI.**

NOMENCLATURE

RSSI	Received signal strength indicator.
LQI	Link quality indicator.
MA	Moving average.
WMA	Weighted moving average.
EWMA	Exponentially weighted moving average.
Max-RSSI	Maximum of RSSI values.
Median-RSSI	Median of RSSI values.
SPI	Serial peripheral interface.
WLAN	Wireless local area network.
WCS and BCS	Worst case and the best case scenarios.
RSSI_mean_j	Mean RSSI value for the zone j.
$\text{RSSI}_{i,j}$	Raw RSSI input value at the sample number i gathered from the zone j.
$\Delta\text{RSSI}_{i,j}$	Different level between mean RSSI and raw RSSI.
N	Number of RSSI samples.
Decision_j	Detection result.
Threshold_j	Predefined threshold.
$\text{RSSI\_mean}_{j(\text{obs})}$	Mean RSSI value from observed signals.
$\text{RSSI\_min}_{j(\text{obs})}$	Minimum RSSI value from observed signals.
C	Constant value.
$\text{RSSI\_input}_{i,j}$	Smoothed RSSI input value.
$W_{1,j}$ and $W_{2,j}$	Weighting factors for proposed methods.
n_j	Window size.
σ_j	Standard deviation.
Receiver_sensitivity	Receiver sensitivity.
α_j	Weighting factor for EWMA.
$\text{Variation\_level}_{1\text{ to }3,j}$	Variation levels.
RSSI_{dBm}	RSSI value in dBm.
RSSI_{dec}	RSSI value as a decimal number.
$\text{RSSI}_{\text{offset}}$	RSSI offset value.
Level_index	Window size index.

Manuscript received May 13, 2018; revised January 1, 2019, April 16, 2019, and May 16, 2019; accepted May 24, 2019. Date of publication June 18, 2019; date of current version August 23, 2019. This work was supported in part by the Visiting Research Fellowships from the University of Aizu, Japan and in part by the Faculty of Engineering, Prince of Songkla University, Thailand, under Grant ENG-62-2-7-02-0254S. *(Corresponding author: Apidet Booranawong.)*

A. Booranawong and N. Jindapetch are with the Department of Electrical Engineering Faculty of Engineering, Prince of Songkla University, Songkhla 90112 Thailand (e-mail: apidet.boo@gmail.com; nattha.s@psu.ac.th).

H. Saito is with the University of Aizu, Aizuwakamatsu 965-8580 Japan (e-mail: hiroshis@u-aizu.ac.jp).

Digital Object Identifier 10.1109/JSYST.2019.2919642

I. INTRODUCTION

DETECTION and tracking of human movements using radio signal strength in indoor wireless networks is a technology, which can be applied in various applications, such as elderly and patient monitoring [1], intrusion detection and tracking [2], human tracking through walls [1], human monitoring and tracking in emergency situations (i.e., during dark periods, smoke events, and fires etc.) [4], human monitoring for controlling autonomous devices [3], [4], and so on. Since in many cases, humans to be tracked cannot carry any device with radio components due to its weight or the effect of the electromagnetic interference, a device-free human detection and tracking system using RSSI signals, which works by monitoring and analyzing the changes in measured RSSI signals of many static links affected by human movements, is developed to fulfill such a requirement [2], [5].

We note that, traditionally, the human detection and tracking technology is a computer vision based, which requires the use of video camera to monitor humans. Although the vision based is an efficient technique as it can retain the records with high resolution, it still has several limitations including cost inefficiency for large-scale deployments, energy consumption, and serious user privacy concerns if it is installed and used in

privacy areas such as bathroom and bedroom (i.e., for elderly care, patient monitoring, and assisted living applications). In addition, the video camera also requires a good lighting area for its accuracy, ineffective in the dark/smoke and has limited view angles. Consequently, recently, a radio frequency-based technique has received research attentions to be employed in the human detection and tracking [1]–[5].

The RSSI information is widely used in a device-free human detection and tracking system because most wireless devices have RSSI circuits built into them. As a result, there is no requirement for an additional hardware. This can help to reduce the hardware cost and the energy consumption of the system [6]. However, the major problem in the use of the RSSI is that the measured RSSI signal is time-varying and unreliable. It generally fluctuates over time due to multipath effects [5], [7]. High variation of the RSSI signal can significantly result in high levels of detection and tracking errors. Consequently, reducing the RSSI variation in the device-free human detection and tracking system to satisfy an acceptance level of the detection and tracking accuracy is required.

Based on prior studies in research literature, the study of the reduction of RSSI variation in a human detection and tracking system is summarized here. In [8], the average method and the exponentially weighted moving average (EWMA) method were applied to measured RSSI signals. Shin *et al.* claimed that, by experiments in an indoor environment, after a filtering process, the RSSI variation was significantly reduced. In [9], by applying the moving average (MA) method and the weighted moving average (WMA) method to measured RSSI signals, the accuracy of the RSSI to distance conversion was properly improved. In [10], a filtering method designed by taking the RSSI and the link quality indicator (LQI) information into consideration was proposed. Experimental results showed that the proposed method in [10] could reduce the RSSI variation around 25%, and the conversion accuracy of the RSSI to the relative distance was significantly improved. However, for the works in [8]–[10], how those filtering methods affected the accuracy of the device-free human detection and tracking system was not the scope of the studies.

In [11], the improvement of RSSI signals in a localization system was proposed. The RSSI signals were filtered using the median method, where the median value in each RSSI signal sequence was continuously determined. Based on the simulation approach, the results showed that the median method could reduce the RSSI variation and improve the localization accuracy. However, the localization system in [11] could be considered as a device-based localization system [5], where objects to be monitored directly carry radio devices. Thus, how the median method effected the device-free detection and tracking system could not be evaluated.

In [12], a comparison of RSSI filtering methods for a device-based indoor localization system was studied through the experiment. The MA, the EWMA, the moving median, and the moving mode as the filtering methods were selected and tested due to the low computational complexity required to use them for filtering RSSI streams in real time [12]. Here, Koledoye *et al.* reported that the MA and the EWMA showed overall high accuracy.

In [13], an RSSI-based method to detect and track an intruder was proposed. An RSSI mean and its standard deviation computed over a predefined number of samples were used to detect the RSSI change caused by the intruder. In [14], a method to detect human movements by processing the standard deviation of the RSSI time series at each time window was proposed. The human was detected when the standard deviation was larger than an optimal threshold. In [15], a study of human detection using radio irregularity for automated people counting was presented. People were detected by considering a probability of the RSSI variation. In [3], an RSSI-based human detection method for residential smart energy systems was introduced. Mrazovac *et al.* demonstrated the performance of their proposed method to detect the human and control the smart power outlets and light switches. Although the works presented in [3] and [13]–[15] proposed the device-free human detection and tracking systems using the RSSI, to reduce the RSSI variation for improving the accuracy was not included in those studies.

In [2], real-time intrusion detection and tracking through distributed RSSI processing was presented. An attenuation of the RSSI affected by an intruder was detected, and the intruder was then located. The EWMA method was also applied to the measured RSSI signals to filter the RSSI variation. Although the work presented in [2] developed the device-free intruder detection and tracking system by taking the RSSI filtering method into consideration, how the EWMA method influenced the sensitivity of the detection and tracking accuracy was not focused.

In [16] (i.e., our previous work), a device-free human detection and tracking system using an RSSI signal was developed. A simple WMA method was used to filter RSSI signals, and a zone selection function for human detection and tracking was also proposed and implemented to increase the detection and tracking accuracy. However, the major objective of the work presented in [16] was to develop the communication protocol and the detection and tracking method, where the development of the RSSI filter was not included in the scope of the study. In this paper, more suitable and efficient filtering methods in terms of accuracy and complexity are further applied, and the zone selection method in [16] is not required. A summary comparison between this paper and the related works is given in Table I.

According to the research gaps introduced earlier, in this paper, adaptive RSSI filtering methods developed by considering both the accuracy as well as the complexity in the device-free human detection and tracking system are presented. The major contributions of our proposed filtering methods are threefold and can be given as follows.

1) First, RSSI variation levels are determined, and RSSI inputs are automatically filtered only when their variations reach a predefined threshold. By this purpose, the computational complexity required by the filtering methods can be saved.
2) Second, RSSI inputs with different variation levels are filtered with different filtering levels adaptively. By this purpose, the human detection and tracking accuracy can be improved.
3) Third, several human movement patterns with different movement directions and speeds are tested to investigate the performance of the proposed filtering methods.

Experimental results demonstrate that, using the proposed methods, the RSSI variation can be properly compensated. The computational complexity defined by the number of mathematical operations is reduced compared to comparative filtering methods (i.e., the well-known and widely-used methods): the MA method, the WMA method, the EWMA method, the maximum method, and the median method. Finally, the system can correctly specify the actual zones where the man is present.

TABLE I
SUMMARY COMPARISON BETWEEN THIS WORK AND THE RELATED WORKS

Ref.	Type of system	Type of study & Test field	Wireless technology	Filtering method	Research issue
[8]	Device-based	Experiment & Indoor	IEEE802.15.4/ZigBee 2.4 GHz	- Average - EWMA	The RSSI filtering methods were applied to improve localization accuracy.
[9]	Device-based	Experiment & Indoor	IEEE802.15.4/ZigBee 2.4 GHz	- MA - WMA	The RSSI filtering methods were applied to improve the accuracy of the RSSI to distance conversion
[10]	Device-based	Experiment & Indoor	IEEE802.15.4/ZigBee 2.4 GHz	- EWMA with RSSI and LQI	The filtering method was proposed to improve the conversion accuracy of the RSSI to the relative distance.
[11]	Device-based	Simulation	-	Moving median	The filtering method was proposed to reduce the RSSI variation and improve the localization accuracy.
[12]	Device-based	Experiment & Indoor	2.4 GHz	- MA - EWMA - Moving median - Moving mode	The comparison of the RSSI filtering methods for a device-based localization system was studied.
[13]	Device-free	Experiment & Indoor	IEEE802.15.4 2.4 GHz	No	The device-free intruder detection method using RSSI was proposed.
[14]	Device-free	Experiment & Indoor	IEEE802.11 b/g/n 2.4 GHz	No	The device-free human detection system was developed.
[15]	Device-free	Experiment & Indoor/outdoor	IEEE802.15.4 2.4 GHz	No	The study of human detection using radio irregularity for automated people counting was presented.
[3]	Device-free	Experiment & Indoor	IEEE802.15.4/ZigBee 2.4 GHz	No	The device-free human detection method using RSSI for residential smart energy systems was introduced.
[2]	Device-free	Experiment & Indoor	IEEE802.15.4/ZigBee 2.4 GHz	EWMA	The device-free intrusion detection and tracking system using RSSI was presented.
[16]	Device-free	Experiment & Indoor	CC2500 transceiver 2.4GHz	WMA	The device-free human detection and tracking system was developed.
This work	Device-free	Experiment & Indoor	CC2500 transceiver 2.4GHz	The proposed adaptive RSSI filtering methods	- The device-free human detection and tracking system using RSSI was developed and tested. - Adaptive RSSI filters designed by considering both the detection/tracking accuracy and the computational complexity were developed. - The adaptive RSSI filters are tested and evaluated in the cases of different human movement patterns and speeds.

The structure of this paper is as follows. Section II describes the human detection and tracking systems including the wireless communication system and the human detection and tracking system. Section III describes the proposed adaptive RSSI filtering methods including the proposed methods 1 and 2. Section IV provides experiments including setup, test scenarios, and comparative methods. Section V provides experimental results and discussion including the accuracy and complexity analysis. We conclude the paper and provide the future work in Section VI.

II. HUMAN DETECTION AND TRACKING SYSTEMS

A. Wireless Communication System

The wireless network presented in this paper is shown in Fig. 1. There are one base station node connected to a computer (the processing center), one receiver node (Rx node ID 0), and three transmitter nodes (Tx node IDs 1, 2, and 3). The Tx and Rx nodes are placed at predefined locations covering the expected detection and tracking area. We note that the illustration in Fig. 1 is also corresponding to our test field described in Section IV.

When the computer wants to detect and track the human in the network, it first notifies the base station node to generate and send a packet, namely the command packet, to each transmitter node sequentially (beginning with the Tx node ID1). The corresponding transmitter node then generates a packet, namely a beacon packet, and sends the beacon packet to the receiver node. Upon receiving the beacon packet, the receiver node immediately reads the RSSI value from the RSSI status register provided by its radio circuit. The receiver node then forward the RSSI value as encapsulated in a packet, namely the data packet, to the base station node. The base station node also transfers the data packet to the computer. Finally, at the computer, the RSSI value from each transmitter node is inserted to the human detection and tracking system.

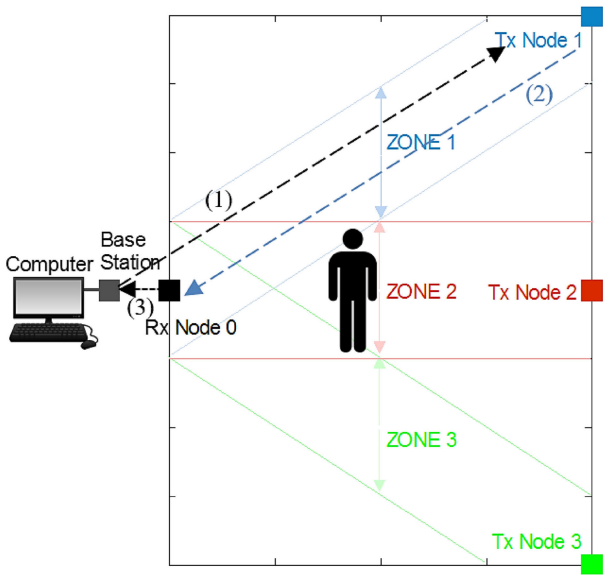

Fig. 1. Wireless network: (1), (2), and (3) refer to the sending of the command packet, the beacon packet, and the data packet, respectively.

We note that, to save the power consumption of wireless nodes and to reduce the signal interference caused in the network, we intend to control the base station node to communicate with each transmitter node sequentially. Thus, the base station node is programmed to communicate with the transmitter node IDs 1, 2, and 3, respectively, and this process is repeated in every iteration. Since a sequential transmission manner is introduced to avoid radio signal interference, this can cause a tradeoff between the communication latency and the communication reliability when there are more transmitters and receivers in large-scale networks. Therefore, such an issue should be considered for further studies. In addition, due to this sequential transmission manner, time

synchronization problems for all transmitter nodes can occur. Thus, optimal solutions for managing this problem should also be developed. Details of the wireless network introduced earlier and its limitations are described in our previous work [16].

B. Human Detection and Tracking System

The human detection and tracking process begins after the computer receives the RSSI values from the transmitter nodes. The main concept of how to detect and track human movements is described here. Generally, without humans in the communication area between the transmitter and the receiver nodes, RSSI values received by the receiver node often fluctuate around their mean. On the other hand, when the human is in the communication area, blocking the radio signal path, the measured RSSI will significantly fluctuate [17], [18]. Thus, the variations in the RSSI values can represent the presence and movement of the human [18], [19]. By this understanding, we use a different level between a mean RSSI value determined during no human presence and a measured RSSI value collected during the test to compare with a predefined threshold (i.e., an appropriate RSSI variation level, which can indicate the human presence) for detecting the human. Detection results from all communication pairs (i.e., Tx 1 and Rx 0 in the zone 1, Tx 2 and Rx 0 in the zone 2, and Tx 3 and Rx 0 in the zone 3, as shown in Fig. 1) are determined simultaneously.

Here, the process of the human detection and tracking is explained. During no human presence in the communication area, the receiver node is assigned to collect the RSSI values from each transmitter node with a predefined number of samples. This set of the RSSI is used to determine the mean RSSI value for the zone j ($\mathrm{RSSI\_mean}_j$, where $j = 1$, 2, and 3) as shown in

$$\mathrm{RSSI\_mean}_j = \frac{1}{N}\sum_{i=1}^{N}\mathrm{RSSI}_{i,j}, \quad \text{where } i = 1 \text{ to } N \tag{1}$$

where $\mathrm{RSSI}_{i,j}$ is the raw RSSI input value at the sample number i gathered from the zone j, and N is the number of RSSI samples to be averaged. It is set to 50 in this paper. We note that to obtain a more accurate $\mathrm{RSSI\_mean}_j$, the number of RSSI samples to be averaged can be set to greater than 50 samples. However, in our experiment, only 50 samples can be properly used. It provides accurate detection and tracking results. During the test, this mean RSSI value is compared to the new RSSI input value ($\mathrm{RSSI}_{i,j}$, where $i > N$). If the subtraction result between them ($\Delta\mathrm{RSSI}_{i,j}$) is smaller than the predefined threshold ($\mathrm{Threshold}_j$) of the zone, it means that there is no human blocking the radio signal path in the zone. Otherwise, the human is in the zone. $\Delta\mathrm{RSSI}_{i,j}$, $\mathrm{Decision}_j$, and $\mathrm{Threshold}_j$ are written by (2)–(4), respectively, as follows:

$$\Delta\mathrm{RSSI}_{i,j} = \mathrm{RSSI\_mean}_j - \mathrm{RSSI}_{i,j}, \quad \text{where } i > N \tag{2}$$

$$\mathrm{Decision}_j = \begin{cases} 0 \text{ (no presence)}, & \text{if} \Delta\mathrm{RSSI}_{i,j} < \mathrm{Threshold}_j \\ 1 \text{ (presence)}, & \text{if } \Delta\mathrm{RSSI}_{i,j} \geq \mathrm{Threshold}_j \end{cases} \tag{3}$$

$$\mathrm{Threshold}_j = \left(\mathrm{RSSI\_mean}_{j(\mathrm{obs})} - \mathrm{RSSI\_min}_{j(\mathrm{obs})}\right) \times \frac{C}{100}. \tag{4}$$

For the threshold in (4), it represents the level of the RSSI variation and equals to the percentage of the different levels between the mean RSSI value ($\mathrm{RSSI\_mean}_{j(\mathrm{obs})}$) and the minimum RSSI value ($\mathrm{RSSI\_min}_{j(\mathrm{obs})}$). $\mathrm{RSSI\_mean}_{j(\mathrm{obs})}$ and $\mathrm{RSSI\_min}_{j(\mathrm{obs})}$ are determined from an observed RSSI signal measured in an offline phase, when the human continuously moves passing each zone. This will be further explained in Section IV. Thus, there are three different thresholds for the zones 1, 2, and 3 to be used. To determine an optimal threshold of each zone, the constant C is varied with nine levels: 0, 12.50, 25, 37.50, 50, 62.50, 75, 87.50, and 100, which refer to 0% to 100% of the different levels between $\mathrm{RSSI\_mean}_{j(\mathrm{obs})}$ and $\mathrm{RSSI\_min}_{j(\mathrm{obs})}$. Through our experiments, we found that the C of 37.50 provides the best detection accuracy; using the smaller value of C cannot classify the difference between human presence and no presence, while using the higher value of C, the human can be detected after the time the man comes to the zone.

We note that details of the human detection and tracking system introduced earlier and its limitations were also presented in our previous work [16], where the method can be efficiently used in the case of one man presented in the wireless network. For the detection and tracking of multiple persons, the method should be further developed.

III. Proposed Adaptive Filtering Methods for RSSI Signals

To improve the detection and tracking accuracy, before the raw RSSI input value ($\mathrm{RSSI}_{i,j}$) is used to compare with $\mathrm{RSSI\_mean}_j$ as presented in (2), $\mathrm{RSSI}_{i,j}$ is first filtered to reduce the noise and its variation by using the proposed filtering methods. We note that, after applying the filtering process, (2) is changed to

$$\Delta\mathrm{RSSI}_{i,j} = \mathrm{RSSI\_mean}_j - \mathrm{RSSI\_input}_{i,j}, \quad \text{where } i > N \tag{5}$$

where, $\mathrm{RSSI\_input}_{i,j}$ is the smoothed RSSI input value which is calculated by taking $\mathrm{RSSI}_{i,j}$ into consideration. The main concept of our proposed filtering methods is that the raw RSSI input value will be filtered only when it has more variation levels (especially during the human presence and movement). If the raw RSSI value is stable in an acceptable level, there is no need to filter it (to reduce the number of computation times of filtering methods). Since the distribution of the measured RSSI values can follow a normal distribution with some mean value ($\mathrm{RSSI\_mean}$) and its standard deviation (σ) in the case of line-of-sight communications [20], [21], in this paper, the raw RSSI input value will be compared with $\mathrm{RSSI\_mean} \pm 2\sigma$ to identify the variation level. In addition, in our proposed filtering methods, the raw RSSI input values with the different variation levels will be filtered with the different degrees of filtering levels. We propose two filtering methods: the proposed methods 1 and 2, as described in the following.

A. Proposed Method 1

In the proposed method 1, $\mathrm{RSSI\_input}_{i,j}$ is determined by (6), shown at the bottom of the next page, where $W_{1,j}$ and $W_{2,j}$ are the weighting factors, and n_j is the number of raw RSSI samples to be averaged (or the window size). The weighting factors are set based on the rule in (7), where $\mathrm{RSSI\_mean}_j$ and σ_j are the RSSI mean value and the standard deviation of the zone j determined from the predefined N RSSI samples during no human presence, as expressed in (1) and (8). By the rule in (7), $\mathrm{RSSI\_mean}_j - 2\sigma_j$ refers to the threshold used to identify the RSSI variation level. Here, if $\mathrm{RSSI}_{i,j}$ is lower than $RSSI\_mean_j - 2\sigma_j$, $W_{1,j}$ and $W_{2,j}$ are then set

to 1 and 0, and the MA function i.e.,$(\mathrm{RSSI}_{i,j} + \mathrm{RSSI}_{i-1,j} + \ldots + \mathrm{RSSI}_{i-n_j+1,j})/n_j$ is considered. On the other hand, the raw RSSI input value is stable. $W_{1,j}$ and $W_{2,j}$ are set to 0 and 1, and $\mathrm{RSSI}_{i,j}$ is directly used as $\mathrm{RSSI\_input}_{i,j}$. We note that 2σ is selected because in a normal distribution, 95.44% of the population is within $\pm 2\sigma$. -2σ is considered because when the human is present in the communication area, blocking the radio signal path, the measured RSSI value will decrease, which is corresponding to the left side of a normal distribution.

Weighting factors

$$= \begin{cases} W_{1,j} = 1 \text{ and } \quad W_{2,j} = 0, \\ \mathrm{RSSI}_{i,j} < (\mathrm{RSSI\_mean}_j - 2\sigma_j) \\ W_{1,j} = 0 \quad \text{and} \quad W_{2,j} = 1, \text{ else} \end{cases}$$

$$\text{where } i > N \tag{7}$$

$$\sigma_j = \sqrt{\frac{1}{N-1}\sum_{i=1}^{N} \left(\mathrm{RSSI}_{i,j} - \mathrm{RSSI\_mean}_j\right)^2} \tag{8}$$

To set the appropriate window size n_j, we use the rule in (9), where n_j depends on the RSSI variation levels. If $\mathrm{RSSI}_{i,j}$ is between $\mathrm{RSSI\_mean}_j - 2\sigma_j$ and $\mathrm{RSSI\_mean}_j - 3\sigma_j$ (representing a small RSSI variation level), n_j is set to $n_{1,j}$. If $\mathrm{RSSI}_{i,j}$ is between $\mathrm{RSSI\_mean}_j - 3\sigma_j$ and $\mathrm{RSSI\_mean}_j - 4\sigma_j$ (a middle RSSI variation level), n_j is set to $n_{2,j}$. Finally, if $\mathrm{RSSI}_{i,j}$ is between $\mathrm{RSSI\_mean}_j - 4\sigma_j$ and Receiver_sensitivity (a high RSSI variation level), n_j is set to $n_{3,j}$, where $n_{3,j}$ is larger than $n_{2,j}$ and $n_{1,j}$, respectively. Here, the larger value of n_j will have a greater smoothing effect to the raw RSSI value, but it requires more computation time for the calculation. In this paper, to find the optimal values of $n_{1,j}$, $n_{2,j}$, and $n_{3,j}$, three different sets of those values are tested; they are equal to (3, 5, 7), (5, 7, 9), and (7, 9, 11), respectively. For Receiver_sensitivity, it is defined as the minimum signal power level required to achieve bit error rate, below which the packet cannot be received. The receiver sensitivity depends on the radio module. Since in this paper, we use the CC2500 transceiver, at the data rate of 500 kb/s, the receiver sensitivity is –83 dBm [22].

$$n_j = \begin{cases} n_{1,j}, & (\mathrm{RSSI\_mean}_j - 3\sigma_j) \\ & \quad \le \mathrm{RSSI}_{i,j} < (\mathrm{RSSI\_mean}_j - 2\sigma_j) \\ n_{2,j}, & (\mathrm{RSSI\_mean}_j - 4\sigma_j) \\ & \quad \le \mathrm{RSSI}_{i,j} \le (\mathrm{RSSI\_mean}_j - 3\sigma_j) \\ n_{3,j}, & \mathrm{Receiver\_sensitivity} \le \mathrm{RSSI}_{i,j} \\ & \quad \le (\mathrm{RSSI\_mean}_j - 4\sigma_j) \end{cases} \tag{9}$$

B. Proposed Method 2

In the proposed method 2, $\mathrm{RSSI\_input}_{i,j}$ is determined by (10). The weighting factors are also set using the rule in (7). Here, if $\mathrm{RSSI}_{i,j}$ is lower than $\mathrm{RSSI\_mean}_j - 2\sigma_j$, the EWMA function (i.e., $\alpha_j \mathrm{RSSI}_{i,j} + (1-\alpha_j)\mathrm{RSSI\_input}_{i-1,j}$) is considered, where α_j is also the weighting factor for the EWMA. By the EWMA, the smoothed RSSI value ($\mathrm{RSSI\_input}_{i,j}$) depends on the previous smoothed value ($\mathrm{RSSI\_input}_{i-1,j}$) and the current raw input value ($\mathrm{RSSI}_{i,j}$) multiplied by α ($0 \le \alpha_j \le 1$). α close to 1 gives high priority to current changes in the input value, while α close to 0 indicates that the previous smoothed value plays a role in the calculation. If $\mathrm{RSSI}_{i,j}$ is higher than $\mathrm{RSSI\_mean}_j - 2\sigma_j$, $\mathrm{RSSI}_{i,j}$ is directly used as $\mathrm{RSSI\_input}_{i,j}$. Here, we note that $\mathrm{RSSI\_input}_{N=50,j} = \mathrm{RSSI\_mean}_j$ in (1).

$$\mathrm{RSSI\_input}_{i,j} = \left(W_{1,j} \times \left(\alpha_j \mathrm{RSSI}_{i,j} + (1-\alpha_j)\,\mathrm{RSSI\_input}_{i-1,j}\right)\right) + \left(W_{2,j} \times \mathrm{RSSI}_{i,j}\right), \quad \text{where } i > N \tag{10}$$

To set the appropriate weighting factor α_j, it also depends on the variation levels of the RSSI values. We use the rule in (11), shown at the bottom of the page. If $\mathrm{RSSI}_{i,j}$ is between $\mathrm{RSSI\_mean}_j - 2\sigma_j$ and $\mathrm{RSSI\_mean}_j - 3\sigma_j$ (a small variation level), α_j is $-0.1667\ (\mathrm{Variation\_level}_{1,j}) + 0.5$. If $\mathrm{RSSI}_{i,j}$ is between $\mathrm{RSSI\_mean}_j - 3\sigma_j$ and $\mathrm{RSSI\_mean}_j - 4\sigma_j$ (a middle variation level), α_j is set to $-0.1667(Variation\_level_{2,j}) + 0.3333$. Finally, if $\mathrm{RSSI}_{i,j}$ is between $\mathrm{RSSI\_mean}_j - 4\sigma_j$ and Receiver_sensitivity (a high variation level), α_j is $-0.1667(\mathrm{Variation\_level}_{3,j}) + 0.1667$.

$\mathrm{Variation\_level}_{1\text{ to }3,j}$ are the variation levels determined by (12)–(14).

$$\mathrm{Variation\_level}_{1,j} = \frac{|\mathrm{RSSI}_{i,j}| - |\mathrm{RSSI\_mean}_j - 2\sigma_j|}{|\mathrm{RSSI\_mean}_j - 3\sigma_j| - |\mathrm{RSSI\_mean}_j - 2\sigma_j|} \tag{12}$$

$$\mathrm{Variation\_level}_{2,j} = \frac{|\mathrm{RSSI}_{i,j}| - |\mathrm{RSSI\_mean}_j - 3\sigma_j|}{|\mathrm{RSSI\_mean}_j - 4\sigma_j| - |\mathrm{RSSI\_mean}_j - 3\sigma_j|} \tag{13}$$

$$\mathrm{Variation\_level}_{3,j} = \frac{|\mathrm{RSSI}_{i,j}| - |\mathrm{RSSI\_mean}_j - 4\sigma_j|}{|\mathrm{Receiver\_sensitivity}| - |\mathrm{RSSI\_mean}_j - 4\sigma_j|} \tag{14}$$

By (11)–(14), α_j is among 0 to 0.5, and it can be divided into three different ranges: $\alpha_j\ \varepsilon(0 \text{ to } 0.1667)$, $\alpha_j\ \varepsilon\ (0.1667 \text{ to } 0.3333)$, and $\alpha_j\ \varepsilon(0.333 \text{ to } 0.5)$, as shown in (15) at the bottom of the next page. The relationship between the range of α_j and the variation level is also illustrated in Fig. 2(a)–(c), where *x* and *y* are the variation level and α_j, respectively. By the proposed method 2, α_j can be automatically and adaptively adjusted depending on the variation levels of the raw RSSI input value.

$$\alpha_j = \begin{cases} -0.1667\,(\mathrm{Variation\_level}_{1,j}) + 0.5, & (\mathrm{RSSI\_mean}_j - 3\sigma_j) \le \mathrm{RSSI}_{i,j} < (\mathrm{RSSI\_mean}_j - 2\sigma_j) \\ -0.1667\,(\mathrm{Variation\_level}_{2,j}) + 0.3333, & (\mathrm{RSSI\_mean}_j - 4\sigma_j) \le \mathrm{RSSI}_{i,j} \le (\mathrm{RSSI\_mean}_j - 3\sigma_j) \\ -0.1667\,(\mathrm{Variation\_level}_{3,j}) + 0.1667, & \mathrm{Receiver\_sensitivity} \le \mathrm{RSSI}_{i,j} \le (\mathrm{RSSI\_mean}_j - 4\sigma_j) \end{cases}, \quad \text{where } i > N \tag{11}$$

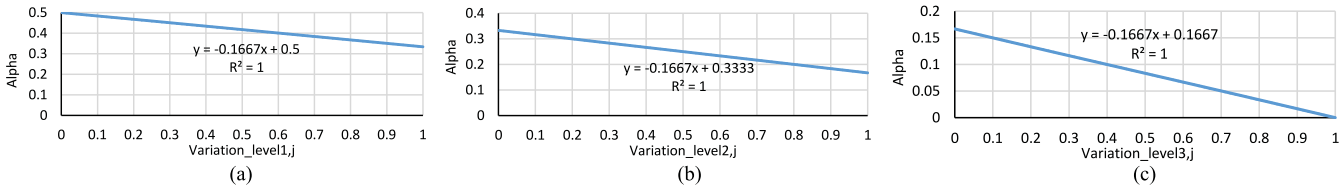

Fig. 2. Relationship between α_j and (a) $\text{Variation\_level}_{1,j}$, (b) $\text{Variation\_level}_{2,j}$, and (c) $\text{Variation\_level}_{3,j}$.

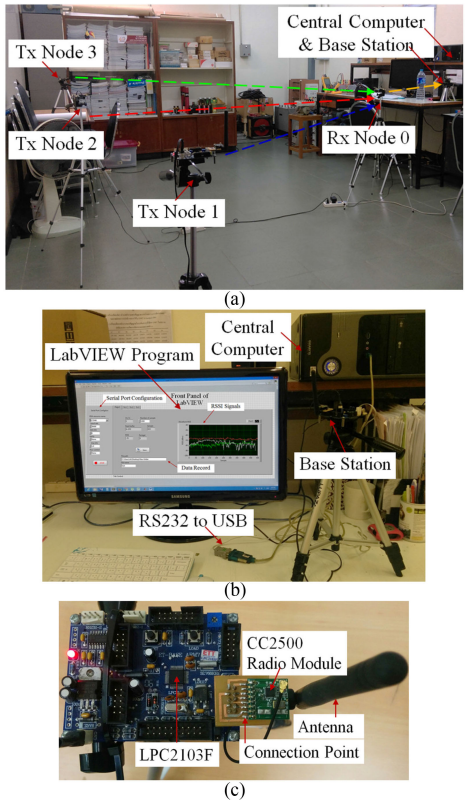

Fig. 3. (a) Test field. (b) Real-time RSSI signals displayed on the computer. (c) Wireless node: the LPC2103F interfacing with the CCC2500.

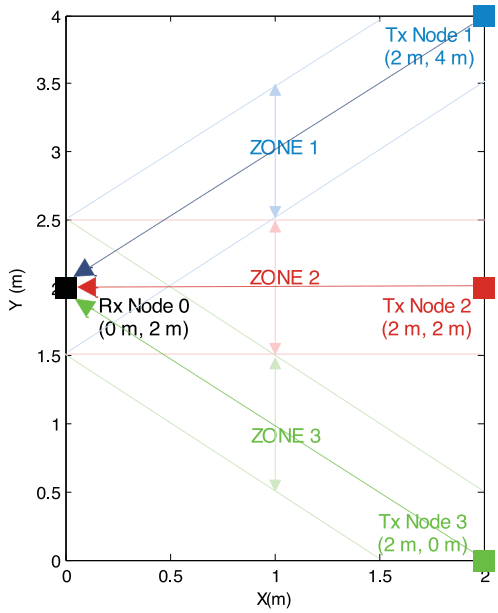

Fig. 4. Layout of the test field.

We note that the maximum value of α_j is set to 0.5 because when there is the variation in the raw RSSI input value, the previous smoothed RSSI value in (10) should have more priority in the calculation than the current raw RSSI value. Thus, α_j below 0.5 is intently considered. In addition, in the proposed method 2, the optimal weighting factor for the EWMA can be automatically and adaptively determined, thus, there is no need to assign the weighting factor during experiments, like the case of the setting of the window size for the MA function in the proposed method 1.

IV. Experiments

A. Experimental Setup

To evaluate the performance of the human detection and tracking system and the proposed filtering methods presented in Sections II and III, experiments have been carried out in a laboratory room at the Department of Electrical Engineering, Prince of Songkla University, Thailand, as shown in Fig. 3. Also, the layout of the test field is illustrated in Fig. 4. The area of the test field is 2.00 m × 4.00 m. There are three transmitter nodes fixed at the positions ($x_1 = 2.00$ m and $y_1 = 4.00$ m), ($x_2 = 2.00$ m and $y_2 = 2.00$ m), and ($x_3 = 2.00$ m and $y_3 = 0.00$ m), respectively, and the receiver node, which is connected to the base station node and the computer, is fixed at the position ($x_4 = 0.00$ m and $y_4 = 2.00$ m). The transmitter and the receiver nodes are kept at the same altitude from the ground at one-meter height. In this test field, the receiver node can forward the data to the base station node with one-hop communications, and the base station node communicates with the computer via an RS232 serial port interface. For real-time RSSI signals, they are collected and displayed on the computer. We note that since the received signal strength depends on the distance between the transmitter and the receiver nodes, to keep the accuracy of the human detection and tracking, RSSI_mean_j and Threshold_j in (1) and (4) should be recalculated if the test environment is changed.

To maintain a level of detection and tracking accuracy, the transmitter and the receiver nodes are intently placed at the defined positions to cover the expected detection and tracking area. Although there are some small spaces among the zones as seen

$$\alpha_j = \begin{cases} -0.1667\,(\text{Variation\_level}_{1,j}) + 0.5 & \rightarrow \alpha_j \varepsilon\,(0.3333 \text{ to } 0.5) \\ -0.1667\,(\text{Variation\_level}_{2,j}) + 0.3333 & \rightarrow \alpha_j \varepsilon\,(0.1667 \text{ to } 0.3333) \\ -0.1667\,(\text{Variation\_level}_{3,j}) + 0.1667 & \rightarrow \alpha_j \varepsilon\,(0 \text{ to } 0.1667) \end{cases} \quad (15)$$

Algorithm 1: RSSI Reading by the CC2500 RF Transceiver.

BEGIN

1: When the CC2500 is in the receiving mode, get the RSSI from the RSSI status register

2: Convert the reading from a hexadecimal number to a decimal number ($\mathrm{RSSI_{dec}}$)

3: IF ($\mathrm{RSSI_{dec}} \geq 128$)$\rightarrow \mathrm{RSSI_{dBm}} = (\frac{\mathrm{RSSI_{dec}} - 256}{2}) - \mathrm{RSSI_{offset}}$

4: ELSE IF ($\mathrm{RSSI_{dec}} < 128$)$\rightarrow \mathrm{RSSI_{dBm}} = (\frac{\mathrm{RSSI_{dec}}}{2}) - \mathrm{RSSI_{offset}}$

END

in Fig. 3(a), in our tests, the movement of human in such spaces can also be detected and tracked. This is because the RSSI signals received by the receiver node still fluctuate due to multipath propagation effects caused by radio reflection, diffraction, and scattering in the indoor environment [5], [17]; the radio signals arrive at the receiver from the transmitter via a variety of paths. However, the optimal placement of the transmitter and receiver pairs and the optimal number of nodes used in the experiment for extending detection and tracking coverage and accuracy are the important research issues, which should be more concerned for the deployment of the transmitters and receivers.

We note that, based on the research literature, several existing works (such as [26] and [27]) related to a device-free detection and tracking system used a high number of nodes in a small test field to obtain high detection accuracy. Thus, they may not be suitable in large-scale networks and in resource-constrained applications. Also, although they are used in a small area, time used for the experimental setup is required, and the hardware cost and power consumption of the system are high as well. By this reason, in the first state of our work, we try to use a small number of nodes deployed in the field to test and verify the system with the proposed filtering methods. In addition, as recommended by [28] and [29], the communication range, signal quality, and detection and tracking accuracy related to optimal node placement are also taken into consideration. In our experiments, the receiver sensitivity of the CC2500 related to node placement issue is considered.

For our devices, the LPC2103F microcontroller interfacing with the CC2500 RF transceiver developed by our research group is employed as the wireless node [22], [23] [see Fig. 3(c)]. The CC2500 is a low-cost 2.4-GHz radio module designed for very low-power wireless applications, and the data rate is set at 500 kb/s. The CC2500 communicates with the LPC2103F via a serial peripheral interface (SPI), which has four input/output pins: master out slave in, master in slave out, slave select, and serial clock. Here, the LPC2103F is the master, and the CC2500 is the slave. Further implementation details of the SPI can be found in [24] and [25]. In addition, since most IEEE 802.11 wireless local area network (WLAN) devices operate on channels 1, 6, and 11, which correspond to the center frequencies 2.412, 2.437, and 2.462 GHz, respectively, in our experiment we intend to configure radio channels of the wireless nodes differently from the radio channels of any WLAN devices, which are available in the EE Department, to avoid signal interference and packet loss.

We note that, RSSI is the measured power of the received radio signal. In the CC2500, the RSSI value in dBm ($\mathrm{RSSI_{dBm}}$) for the selected channel can be read using the procedure as shown in Algorithm 1, where $\mathrm{RSSI_{dec}}$ is the RSSI value as a decimal number, and the $\mathrm{RSSI_{offset}}$ is the offset value corresponding to the data rate. The $\mathrm{RSSI_{offset}}$ is 72 in this paper, since the data rate is set at 500 kb/s. Here, the raw RSSI value ($\mathrm{RSSI_{dBm}}$) is the input for the proposed filtering methods presented in Section III and the human detection and tracking process.

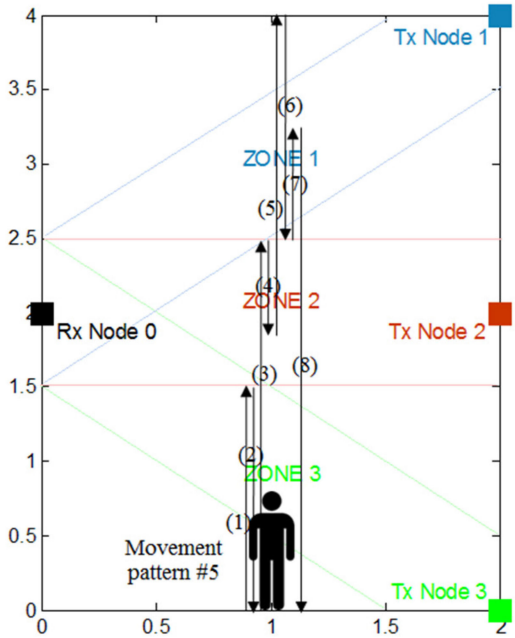

Fig. 5. Example of the movement pattern #5.

B. Test Scenarios

There are five different test scenarios of human movement patterns to be test in the test field. The detail of each movement pattern 1–5 is described as follows.

1) Pattern #1: The man continuously walks in the test field, passing the zones 3, 2, and 1, respectively.
2) Pattern #2: The man walks passing the zones 3, 2, and 1, respectively, and during walking he also stops at each zone for a period of time.
3) Pattern #3: The man continuously walks passing the zones 3, 2, and 1, respectively. Then, he walks back to the starting point (passing the zones 1 to 3, respectively).
4) Pattern #4: The man runs, with the speed higher than walking, passing the zones 3, 2, and 1, respectively. Note that walking/running speeds are 1 and 3 m/s approximately.
5) Pattern #5: The man freely walks and sometimes stops in the zone; he walks passing the zones 3, 3, 3, 2, 2, 2, 1, 1, 1, 2, and 3, respectively (see an example of walking directions indicated by numbers (1) to (8) in Fig. 5).

We define that the movement pattern #1 is for determining the predefined thresholds in (4) setting for the zones 1, 2, and 3. The RSSI signals from this case are the observed signals measured in the offline phase. We note that although the movement patterns described earlier are regular, such movement patterns can be seen in many applications. For examples, people walk across the corridor inside buildings, and elderly people move from one room to another room in their houses. In addition, as mentioned before, the transmitter and receiver nodes are kept at the same altitude from the ground at 1-m height. Thus, false detection can be presented in some scenarios. For example, children and pets move passing the tracking area. Therefore, to prevent this

TABLE II
OPTIMAL WINDOW SIZE (n_j) OR THE WEIGHTING FACTOR (α_j) OF EACH FILTERING METHOD AT THE DETECTION AND TRACKING ACCURACY 100%

Movement Pattern	Optimal window size (n_j) or weighting factor (α_j) of each filtering method						
	MA	WMA	EWMA	Max-RSSI	Median-RSSI	Proposed method 1	Proposed method 2
#1	7	7	0.3	9	7	$n_j = (3, 5, 7)$	$\alpha_j \in (0 \text{ to } 0.5)$
#2	5	5	0.3	5	5	$n_j = (3, 5, 7)$	$\alpha_j \in (0 \text{ to } 0.5)$
#3	5	5	0.3	5	7	$n_j = (3, 5, 7)$	$\alpha_j \in (0 \text{ to } 0.5)$
#4	5	5	0.3	5	5	$n_j = (3, 5, 7)$	$\alpha_j \in (0 \text{ to } 0.5)$
#5	9	9	0.1	9	9	$n_j = (5, 7, 9)$	$\alpha_j \in (0 \text{ to } 0.5)$

situation, in the future work, such an issue should be taken into consideration. Here, two different layers (top and bottom layers) of the transmitter and receiver pairs can be included in the experimental setup to classify the difference between children/pets and adults.

C. Comparative Filtering Methods

The MA method, the WMA method, the EWMA method, the maximum of the RSSI values (Max-RSSI), and the median of the RSSI values (Median-RSSI) as the well-known and widely-used filtering methods [9], [10], [12] are selected and compared with our proposed methods. By this purpose, how well the proposed methods 1 and 2 can reduce the RSSI variation and improve the accuracy and complexity of the system compared with other solutions can be investigated. The smoothed RSSI input values by the MA, the WMA, the EWMA, the Max-RSSI, and the Median-RSSI are defined, respectively, in (16)–(20), shown at the bottom of the this page.

In this paper, in (16), (17), (19), and (20), the window size n_j is varied with five levels during the experiments: 3, 5, 7, 9, and 11, respectively. In (17), the WMA assigns higher weight to more recent input data than the past ($W_1 > W_2 > \cdots > W_{n_j}$). Thus, if the n_j is set to 5 for instance, W_1 to W_5 are set to 5, 4, 3, 2, and 1, respectively. Finally, in (18), the α_j assigned for the EWMA is also varied with five levels: 0.1, 0.3, 0.5, 0.7, and 0.9, respectively.

V. RESULTS AND DISCUSSION

A. Detection and Tracking Accuracy

The optimal n_j or α_j of each filtering method at the detection and tracking accuracy 100% is given in Table II. The detection and tracking accuracy 100% means that the method can correctly specify the actual zones of the man's presence, as described in the test scenario section. Here, the results show that the MA and the WMA provide the same results; the optimal n_j, which give the detection and tracking accuracy 100% are 5, 7, and 9. In the EWMA, the optimal α_j are 0.1 and 0.3. In the Max-RSSI and the Median-RSSI, the optimal n_j is also among 5 and 9.

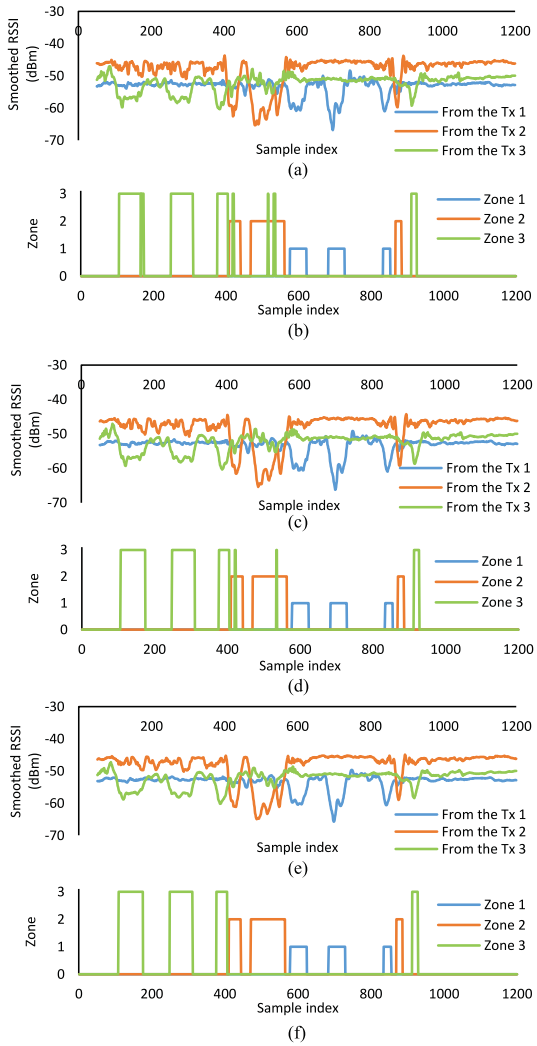

Fig. 6. Smoothed RSSI signals by the MA and the detection and tracking results of the movement pattern #5. (a) and (b) Window size of 5. (b) Detection and tracking results: the MA with the window size of 5. (c) and (d) Window size of 7. (e) and (f) Window size of 9.

$$\text{RSSI\_input}_{i,j} = \frac{(\text{RSSI}_{i,j}) + (\text{RSSI}_{i-1,j}) + \cdots + (\text{RSSI}_{i-n_j+1,j})}{n_j}, \quad \text{where } i > N \tag{16}$$

$$\text{RSSI\_input}_{i,j} = \frac{(W_1 \times \text{RSSI}_{i,j}) + (W_2 \times \text{RSSI}_{i-1,j}) + \cdots + (W_n \times \text{RSSI}_{i-n_j+1,j})}{W_1 + W_2 + \cdots + W_{n_j}}, \quad \text{where } i > N \tag{17}$$

$$\text{RSSI\_input}_{i,j} = \alpha_j \text{RSSI}_{i,j} + (1 - \alpha_j)\,\text{RSSI\_input}_{i-1,j}, \quad \text{where } i > N \text{ and } \text{RSSI\_input}_{N,j} = \text{RSSI\_mean}_j \tag{18}$$

$$\text{RSSI\_input}_{i,j} = \text{Maximum of } (\text{RSSI}_{i,j}, \text{RSSI}_{i-1,j}, + \cdots + \text{RSSI}_{i-n_j+1,j}), \quad \text{where } i > N \tag{19}$$

$$\text{RSSI\_input}_{i,j} = \text{Median of } (\text{RSSI}_{i,j}, \text{RSSI}_{i-1,j}, + \cdots + \text{RSSI}_{i-n_j+1,j}), \quad \text{where } i > N \tag{20}$$

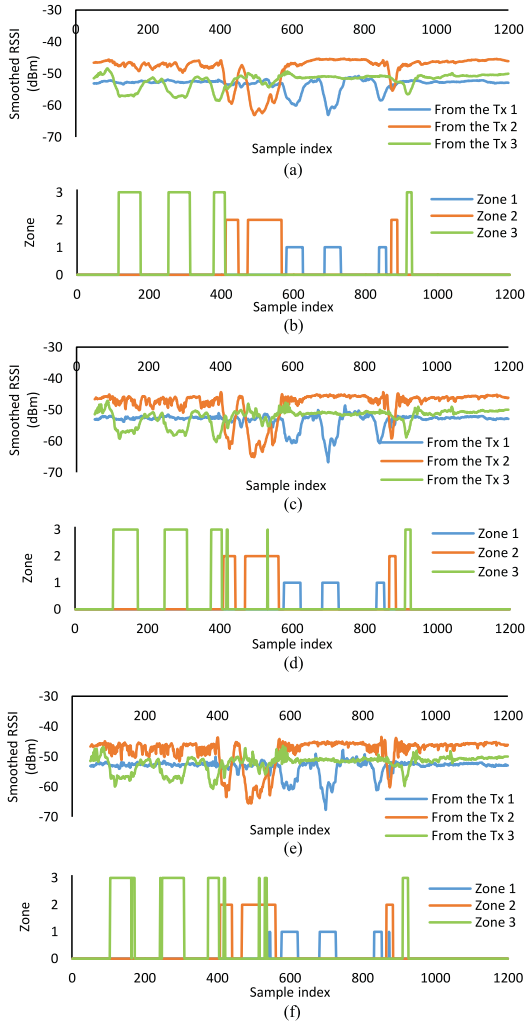

Fig. 7. Smoothed RSSI signals by the EWMA and the detection and tracking results of the movement pattern #5. (a) and (b) Weighting factor of 0.1. (c) and (d) Weighting factor of 0.3. (e) and (f) Weighting factor of 0.5.

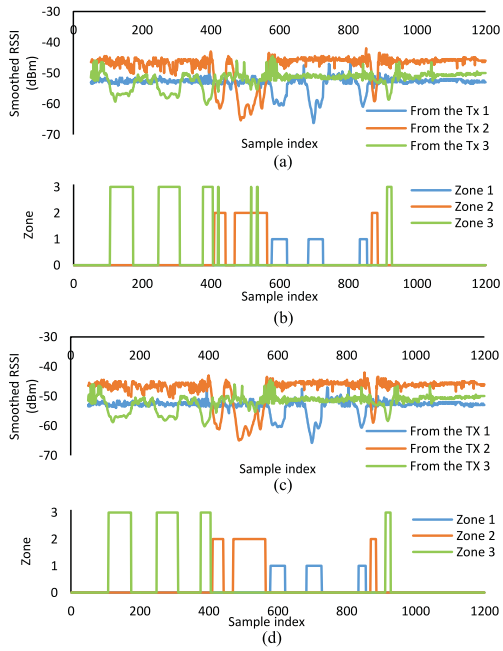

Fig. 8. Smoothed RSSI signals by the proposed method 1 and the detection and tracking results of the movement pattern #5. (a) and (b) $n_j = (3,\ 5,\ 7)$. (c) and (d) $n_j = (5,\ 7,\ 9)$.

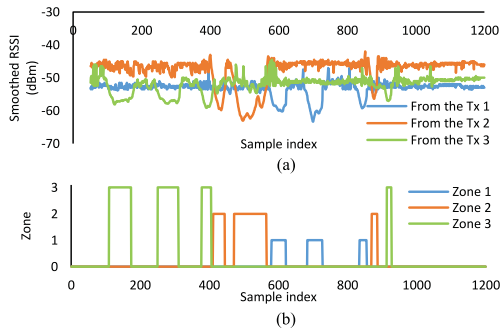

Fig. 9. Smoothed RSSI signals by the proposed method 2 and the detection and tracking results of the movement pattern #5. (a) and (b) $\alpha_j \in (0 \text{ to } 0.5)$.

However, in some cases (i.e., movement patterns #1 and #3), the Max-RSSI and the Median-RSSI use higher n_j than the MA and the WMA.

For the proposed method 1, the optimal range of the window sizes $[n_j = (3,\ 5,\ 7), (5,\ 7,\ 9)]$ is the range that covers the optimal window sizes provided by the MA. Also, in the proposed method 2, the optimal range of the weighting factors $(\alpha_j \in (0\ to\ 0.5))$ covers the range of the optimal weighting factors provided by the EWMA.

The results also indicate that although the MA, the WMA, the EWMA, the Max-RSSI, the Median-RSSI, and the proposed method 1 can achieve the detection and tracking accuracy 100%, the optimal window sizes and the optimal weighting factors are not automatically determined and set during the experiments. On the other hand, such an issue is not a problem for the case of the proposed method 2, since the optimal weighting factors are automatically and adaptively determined based on the RSSI variation levels as presented in (11)–(15).

Examples of the smoothed RSSI signals determined by the MA (with n_j of 5, 7, and 9), the EWMA (with α_j of 0.1, 0.3, and 0.5), the proposed method 1 (with $\mathrm{n_j} = (3, 5, 7), (5, 7, 9)$), the proposed method 2 (with $\alpha_j \in (0 \text{ to } 0.5)$), and the detection and tracking results of the movement pattern #5 are shown in Figs. 6–9, respectively. Note that, for the detection and tracking results, the zone number is displayed when the detection result by threshold described in (3) is 1.

Here, the results demonstrate that the MA with the n_j of 9, the EWMA with the α_j of 0.1, the proposed method 1 with $n_j = (5,\ 7,\ 9)$, and the proposed method 2 with $\alpha_j \in (0 \text{ to } 0.5)$ can support the human detection and tracking method to achieve the accuracy 100% (this correlates with the results in Table II).

The results also show that, for the proposed methods 1 and 2, the raw RSSI input values are filtered only when they have high variations, especially during the human presence and movement in the test field (see the variation of the smoothed RSSI signals in Figs. 8 and 9, the RSSI variation is more decreased during the human presence). This result represents the operation of the proposed methods with the rules in (7), (9), and (11), as introduced in Section III. Unlike the MA method with the window size of 9 and the EWMA with the weighting factor of 0.1, as seen in Figs. 6(e) and (f), and 7(a) and (b), all RSSI samples are filtered.

In Fig. 10, we also show the raw RSSI signals of the movement pattern #5 and the results without applying filtering methods (i.e., only the method in Section II is considered). Here, the

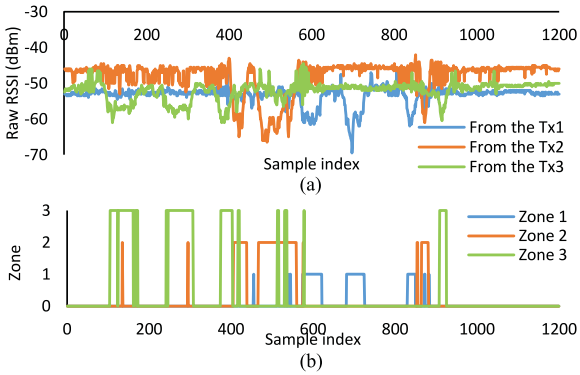

Fig. 10. Raw RSSI signals and the detection and tracking results of the movement pattern #5. (a) and (b) Without applying any filtering methods.

TABLE III
ACTUAL NUMBER OF TIMES THE MAN IS IN THE ZONE

Zones	Movement Pattern				
	#1	#2	#3	#4	#5
1	1	1	2	1	3
2	1	1	2	1	3
3	1	1	2	1	4

TABLE IV
DETECTION AND TRACKING RESULTS BY THE SYSTEM WITH METHOD 2

Zones	Movement Pattern				
	#1	#2	#3	#4	#5
1	1	1	2	1	3
2	1	1	2	1	3
3	1	1	2	1	4

TABLE V
DELIVERY RATIO OF THE DATA PACKETS

Pattern	% Packet Delivery Ratio (from the Transmitter node ID)		
	1	2	3
#1	99.750	100.00	100.00
#2	99.500	99.750	99.750
#3	99.830	99.830	99.830
#4	99.500	100.00	100.00
#5	99.750	99.830	99.750

results show that the system cannot correctly specify the actual zones of the man's presence. For examples, at the RSSI sample indexes 531 to 536, the results indicate that the man is in the zones 2 and 3 at the same time. Similarly, the zones 1 and 2 are simultaneously selected and displayed during the RSSI indexes 872–875. These guarantee the efficiency of the filtering methods, to reduce the RSSI variation and also to correctly specify the actual zone (as seen in Figs. 6–9). This result shows the significance and the contribution of the proposed filtering methods.

Table III gives the actual number of times the man is in the zone of each movement pattern (as presented in the test scenario section), and Table IV illustrates the number of times the system with the proposed method 2 can detect and track the man in the zone. The experimental results confirm that the system with the proposed method 2 can correctly specify the actual zones of the man's presence, in all cases of the movement patterns.

We note that Table V illustrates the delivery ratio of data packets, which is the ratio of the total number of packets received at the base station to the total number of packets sent by the receiver. As explained in Section II, the data packet contains the RSSI value that the receiver reads from its radio circuit. Here, Table V indicates the successful data transmission; the delivery ratio is nearly 100% in all cases.

TABLE VI
NUMBER OF TIMES THE FILTERING METHOD RUNS EACH MATHEMATICAL OPERATION

Filtering Method	The number of times the filtering method runs each mathematical operation
MA; (16)	▪ WCS and BCS $+ = (\text{window size} - 1) \times (NS - 50)$ $/ = 1 \times (NS - 50)$ Note: the first 50 RSSI samples are used to find $RSSI\_mean_j$. Thus, the MA starts at the sample 51.
WMA; (17)	▪ WCS and BCS $+ = (\text{window size} - 1) \times (NS - 50)$ $\times = (\text{window size}) \times (NS - 50)$ $/ = 1 \times (NS - 50)$
EWMA; (18)	▪ WCS and BCS $+ \text{ and } - = 1 \times (NS - 50)$ $\times = 2 \times (NS - 50)$
Max-RSSI; (19)	▪ WCS and BCS $\text{comparison} = (\text{window size} - 1) \times (NS - 50)$
Median-RSSI; (20)	▪ WCS and BCS $\text{comparison} = (\text{window size} \times Level\_index) \times (NS - 50)$ Note: $Level\_index$ 1, 2, 3, 4, and 5 refer to the window sizes of 3, 5, 7, 9, and 11, respectively.
Proposed method 1; (6), (7) and (9)	▪ WCS $+ = (\text{Max. window size} - 1) \times (NS - 50)$ $/ = 1 \times (NS - 50)$ $\text{comparison} = (NS - 50) + (NS - 50) + (NS - 50)$ Note: in WCS, $W_{1,j}$ and $W_{2,j}$ in (6) are 1 and 0, respectively, $n_{3,j}$ in (9) is corresponding to the maximum window size, and the comparisons are from (7) (for one time) and (9) (for two times). ▪ BCS $\text{comparison} = (NS - 50)$ Note: in BCS, $W_{1,j}$ and $W_{2,j}$ are 0 and 1, respectively, and the comparison is from (7) (for one time).
Proposed method 2; (10), (7), and (11) to (14)	▪ WCS $+ = 2 \times (NS - 50)$ $- \text{ and } \times = 3 \times (NS - 50)$ $/ = 1 \times (NS - 50)$ $\text{comparison} = (NS - 50) + (NS - 50) + (NS - 50)$ Note: in WCS, $W_{1,j}$ and $W_{2,j}$ in (10) are 1 and 0, respectively, one of the sub-functions in (11) is selected, and the comparisons are from (7) (for one time) and (11) (for two times). ▪ BCS $\text{comparison} = (NS - 50)$ Note: in BCS, $W_{1,j}$ and $W_{2,j}$ are 0 and 1, respectively, and the comparison is from (7) (for one time).

WCS: the worst case scenario, BCS: the best case scenario.

TABLE VII
EXAMPLES OF THE NUMBER OF TIMES THAT THE FILTERING METHOD RUNS EACH MATHEMATICAL OPERATION TO PROCESS THE MOVEMENT PATTERN #5

(a) The worst case scenario

Operation	MA	WMA	EWMA	Max-RSSI	Median-RSSI	Proposed 1	Proposed 2
+	9200	9200	1150	-	-	**9200**	**2300**
−	-	-	1150	-	-	-	**3450**
×	-	10350	2300	-	-	-	**3450**
/	1150	1150	-	-	-	**1150**	**1150**
comparison	-	-	-	9200	41400	**3450**	**3450**

(b) The best case scenario

Operation	MA	WMA	EWMA	Max-RSSI	Median-RSSI	Proposed 1	Proposed 2
+	9200	9200	1150	-	-	**1150**	**1150**
−	-	-	1150	-	-	-	**1150**
×	-	10350	2300	-	-	-	**1150**
/	1150	1150	-	-	-	**1150**	**1150**
comparison	-	-	-	9200	41400	**1150**	**1150**

B. Complexity

In order to compare the computational cost of each filtering method, the amount of mathematical operations (i.e., summations (+), subtractions (−), multiplications (×), divisions (/), and comparisons) required by each method are determined. This is very useful for finding the most appropriate filtering method, which has the balance between the complexity and the accuracy.

Table VI gives the number of times the filtering method runs each mathematical operation (in a general form) both in the worst case and the best case scenarios, where NS is the number of RSSI samples, and 50 represents the RSSI samples (or N) used to determine RSSI_mean_j as mentioned in Section II (for example, in the movement pattern #5, NS is 1200 samples, as seen in Figs. 6–9, and the first 50 samples are used to find RSSI_mean_j). We note that the worst case means that all RSSI samples after $i > N$ are filtered, while the best case (for the

TABLE VIII
NUMBER OF TIMES THE FILTERING METHOD RUNS EACH MATHEMATICAL OPERATION TO PROCESS THE MOVEMENT PATTERNS #1 TO #5

(a) The movement pattern #1

Operation	Number of times that the filtering method runs the operation						
	MA	WMA	EWMA	Max-RSSI	Median-RSSI	Proposed 1	Proposed 2
+	6300	6300	1050	-	-	1812	778
−	-	-	1050	-	-	-	1167
×	-	7350	2100	-	-	-	1167
/	1050	1050	-	-	-	389	389
comparison	-	-	-	8400	37800	1978	1978
Total	**7350**	**14700**	**4200**	**8400**	**37800**	**4179**	**5479**

(b) The movement pattern #2

+	4200	4200	1050	-	-	2050	768
−	-	-	1050	-	-	-	1152
×	-	5250	2100	-	-	-	1152
/	1050	1050	-	-	-	384	384
comparison	-	-	-	4200	10500	1968	1968
Total	**5250**	**10500**	**4200**	**4200**	**10500**	**4402**	**5424**

(c) The movement pattern #3

+	6600	6600	1650	-	-	1630	694
−	-	-	1650	-	-	-	1041
×	-	8250	3300	-	-	-	1041
/	1650	1650	-	-	-	347	347
comparison	-	-	-	6600	16500	2494	2494
Total	**8250**	**16500**	**6600**	**6600**	**16500**	**4471**	**5617**

(d) The movement pattern #4

+	4200	4200	1050	-	-	770	318
−	-	-	1050	-	-	-	447
×	-	5250	2100	-	-	-	447
/	1050	1050	-	-	-	159	159
comparison	-	-	-	4200	10500	1518	1518
Total	**5250**	**10500**	**4200**	**4200**	**10500**	**2447**	**2889**

(e) The movement pattern #5

+	27600	27600	3450	-	-	5628	1594
−	-	-	3450	-	-	-	2391
×	-	31050	6900	-	-	-	2391
/	3450	3450	-	-	-	797	797
comparison	-	-	-	27600	124200	5194	5194
Total	**31050**	**62100**	**13800**	**27600**	**124200**	**11619**	**12367**

The results in Table VIII are determined from three RSSI signals (i.e., RSSI signals from the Tx 1, Tx 2, and Tx 3), and at the detection and tracking accuracy 100%.

proposed methods 1 and 2) means that all samples after $i > N$ have the value higher than $\mathrm{RSSI\_mean}_j - 2\sigma_j$, and such RSSI samples are not filtered.

Table VII also illustrates examples of the number of times the filtering methods run each mathematical operation to process the movement pattern #5 both in the worst case and the best case scenarios. We assume that: 1) NS is 1200 samples; 2) the window size for the MA, the WMA, the Max-RSSI, and the Median-RSSI methods is 9; 3) the maximum window size for the proposed method 1 is 9; 4) the weighting factor for the EWMA and the proposed method 2 is 0.1.

Here, the results from Tables VI and VII can be summarized that, in the worst case scenario, the proposed methods 1 and 2 use some mathematical operations higher than the comparative methods. However, in the best case scenario, they use the operations equal or smaller than others.

The number of times that the filtering method runs each mathematical operation to process the RSSI signals for the movement patterns #1 to #5 is also reported in Table VIII, where the results are determined from three RSSI signals (i.e., RSSI signals from the Tx 1, Tx 2, and Tx 3) and at the detection and tracking accuracy of 100% (i.e., the optimal window sizes and the optimal weighting factors are from Table II). The experimental results indicate that, mostly, the proposed methods use lower mathematical operations than other comparative filtering methods.

Examples of the calculation in Table VIII are also illustrated in the following. We explain only four cases of the calculation (for the movement pattern #1): the operation $+$ by the MA, the operation $+$ by the proposed methods 1 and 2, and the comparison operation by the proposed methods 1 and 2. For other values provided in Table VIII, they can be calculated based on the same concept.

1) Example 1: The MA uses the operation $+$ of 6300 times. It is calculated from $(\mathrm{window\ size} - 1) \times (NS - 50)$ (in Table VI). Since the optimal window size at the detection and tracking accuracy 100% in Table II is 7 and there are 400 RSSI samples (or NS) from each RSSI signal in the case of the movement pattern #1, the operation $+$ is $(7 - 1) \times (400 - 50) = 2100$. Note that there are 400, 400, 600, 400, and 1200 samples from each RSSI signal in the cases of the patterns #1 to #5, respectively. Thus, since there are three RSSI signals, the total operation $+$ is $3 \times 2100 = 6300$.

2) Example 2: The proposed method 2 uses the operation $+$ of 778 times. It is calculated from $2 \times (NS - 50)$ (WCS in Table VI). However, in this case, the NS should be re-determined based on the actual experiments. There are 103, 181, and 105 times that $\mathrm{RSSI}_{i,j}$ is lower than $RSSI\_mean_j - 2\sigma_j$ for the RSSI signals from the Txs 1, 2, and 3. Thus, the total operation $+$ is $(2 \times 103) + (2 \times 181) + (2 \times 105) = 778$.

3) Example 3: The proposed method 1 uses the operation $+$ of 1812 times. It is calculated from $(\mathrm{Max.\ window\ size} - 1) \times (NS - 50)$ (WCS in Table VI). Because the optimal window size by this method is among (3, 5, 7) as seen in Table II, the NS should also be re-determined. Here, for the signal from the Tx1, there are 103 times that $\mathrm{RSSI}_{i,j}$ is lower than $\mathrm{RSSI\_mean}_j - 2\sigma_j$ including 30 times for the window size $= 3$, 0 time for the window size $= 5$, and 73 times for the window size $= 7$. For the signal from the Tx2,

there are 181 times including 68 times for the window size = 3, 0 time for the window size = 5, and 113 times for the window size = 7. Finally, for the signal from the Tx3, there are 105 times including 25 times for the window size = 3, 15 times for the window size = 5, and 65 times for the window size = 7. Thus, the total operation + is $[((3-1)\times 30)+((5-1)\times 0)+((7-1)\times 73)]+[((3-1)\times 68)+((5-1)\times 0)+((7-1)\times 113)]+[((3-1)\times 25)+((5-1)\times 15)+((7-1)\times 65)]=1812$.

4) Example 4: The proposed methods 1 and 2 use the comparison operation of 1978 times. It is calculated from $(NS-50)+(NS-50)+(NS-50)$ (WCS in Table VI). Here, it can be divided into two cases: the comparison is 3 times for the samples, which have lower values than $\mathrm{RSSI\_mean}_j - 2\sigma_j$ [one time from the rule in (7) and two times from the rule in (9) or (11)], and the comparison is 1 time for the samples, which have higher values than $\mathrm{RSSI\_mean}_j - 2\sigma_j$ [one time from the rule in (7)]. Thus, the total operation is $[(3\times 103)+(3\times 181)+(3\times 105)]+[(1\times(400-103))+(1\times(400-181))+(1\times(400-105))]=1978$.

VI. Conclusion

In this paper, adaptive filtering methods for RSSI signals in a human detection and tracking system are developed and tested. In our proposed methods, to reduce the computational complexity, the RSSI variation level is determined, and the RSSI inputs are automatically filtered only when they have high variation levels. To increase the detection and tracking accuracy, the RSSI inputs with different variation levels are filtered with different filtering levels adaptively. The results show that, by applying the proposed methods, the RSSI variation can be appropriately reduced, and the system can correctly specify the actual zones of the man's presence in all cases of the movement patterns. In the future work, complex human movement patterns in different environments should be tested. Developing communication protocols to support multiple wireless links in large-scale wireless networks, and developing tracking and RSSI filtering methods to support multiple human movements are also required. As mentioned in Section IV, the optimal placement of transmitters and receivers for extending detection/tracking coverage and accuracy is also one of the important issues, which should be considered when designing and developing the device-free detection and tracking system.

References

[1] O. Kaltiokallio, M. Bocca, and N. Patwari, "Follow @grandma: Long-term device-free localization for residential monitoring," in *Proc. IEEE 37th Conf. Local Comput. Netw. Workshops*, 2012, pp. 991–998.

[2] O. Kaltiokallio and M. Bocca, "Real-time intrusion detection and tracking in indoor environment through distributed RSSI processing," in *Proc. IEEE 17th Conf. Embedded Real-Time Comput. Syst. Appl.*, 2011, pp. 61–70.

[3] B. Mrazovac, M.Z. Bjelica, D. Kukolj, B.M. Todorovic, and D. Samardzija, "A human detection method for residential smart energy based on Zigbee RSSI changes," *IEEE Trans. Consum. Electron.*, vol. 58, no. 3, pp. 819–824, Aug. 2012.

[4] A. Booranawong, W. Teerapabkajorndet, and C. Limsakul, "Energy consumption and control response evaluations of AODV routing in WSANs for building-temperature control," *Sensors*, vol. 13, no. 7, pp. 8303–8330, 2013.

[5] N. Patwari and J. Wilson, "RF sensor networks for device-free localization: Measurements, models, and algorithms," *Proc. IEEE*, vol. 98, no. 11, pp. 1961–1973, Nov. 2010.

[6] Q. Lei, H. Zhang, H. Sun, and L. Tang, "A new elliptical model for device-free localization," *Sensors*, vol. 16, no. 4, pp. 1–12, 2016.

[7] A. Booranawong and W. Teerapabkajorndet, "Impact of radio propagation on the performance of directed diffusion routing in mobile wireless sensor networks," in *Proc. Int. Conf. Embedded Syst. Intell. Technol.*, 2009.

[8] S.C. Shin, B.R. Son, W.G. Kim, and J.G. Kim, "ERFS: Enhanced RSSI value filtering schema for localization in wireless sensor networks," in *Proc. Wireless Sensor Actor Netw. II*, 2008, pp. 245–256.

[9] Q. Dong and W. Dargie, "Evaluation of the reliability of RSSI for indoor localization," in *Proc. Int. Conf. Wireless Commun. Underground Confined Areas*, 2012, pp. 1–6.

[10] S.J. Halder and W. Kim, "A fusion approach of RSSI and LQI for indoor localization system using adaptive smoothers," *J. Comput. Netw. Commun.*, vol. 2012, 2012, Art. no. 790374.

[11] J. Chen, H. Qian, and X. Yan, "Localization algorithm using improved RSSI," *J. Inf. Comput. Sci.*, vol. 10, no. 15, pp. 4809–4817, 2013.

[12] M. A. Koledoye, D. D. Martini, S. Rigoni, and T. Facchinetti, "A comparison of RSSI filtering techniques for range-based localization," in *Proc. 23rd IEEE Int. Conf. Emerg. Technol. Factory Autom.*, 2018, pp. 761–767.

[13] S. Hussain, R. Peters, and D.L. Silver, "Using received signal strength variation for surveillance in residential areas," *Proc. SPIE*, vol. 6973, pp. 1–6, 2008.

[14] F. Soldovieri and G. Gennarelli, "Exploitation of ubiquitous Wi-Fi devices as building blocks for improvised motion detection systems," *Sensors*, vol. 16, no. 3, pp. 1–13, 2016.

[15] P.W.Q. Lee, W.K.G. Seah, H.P, Tan, and Z.X. Yao, "Wireless sensing without sensors–An experimental study of motion/intrusion detection using RF irregularity," *J. Meas. Sci. Technol.*, vol. 21, no. 2, 2010.

[16] A. Booranawong, N. Jindapetch, and H. Saito, "A system for detection and tracking of human movements using RSSI signals," *IEEE Sensor J.*, vol. 18, no. 6, pp. 2531–2544, Mar. 2018.

[17] A.Y. Chapre, P. Mohapatra, S. Jha, and A. Seneviratne, "Received signal strength indicator and its analysis in a typical WLAN system," in *Proc. 38th Annu. IEEE Conf. Local Comput. Netw.*, 2013, pp. 304–307.

[18] K. Kaemarungsi and P. Krishnamurthy, "Properties of indoor received signal strength for WLAN location fingerprinting," in *Proc. 1st Annu. Int. Conf. Mobile Ubiquitous Syst., Netw. Services*, 2004, pp. 14–23.

[19] W.C. Lin, W.K.G. Seah, and W. Li, "Exploiting radio irregularity in the Internet of Things for automated people counting," in *Proc. 22nd IEEE Int. Symp. Personal, Indoor Mobile Radio Commun.*, 2011, pp. 1015–1019.

[20] J. Small, A. Smailagic, and D.P. Siewiorek, "Determining user location for context aware computing through the use of a wireless LAN infrastructure." [Online]. Available: http://www-2.cs.cmu.edu/~aura/docdir/small00.pdf

[21] K. Kaemarungsi and P. Krishnamurth, "Properties of indoor received signal strength for WLAN location fingerprinting," in *Proc. 1st Annu. Int. Conf. Mobile Ubiquitous Syst., Netw. Services*, 2004, pp. 14–23.

[22] T. Instrument, CC2500 datasheet. [Online]. Available: http://www.ti.com.cn/cn/lit/ds/swrs040c/swrs040c.pdf

[23] B. Rattanalert, W. Jindamaneepon, K. Sengchuai, A. Booranawong, and N. Jindapetch, "Problem investigation of min-max method for RSSI based indoor localization," in *Proc. 12th Int. Conf. Elect. Eng./Electron., Comput., Telecommun. Inf. Technol.*, 2015, pp. 1–5.

[24] L. D. Yang, "Implementation of a wireless sensor network with EZ430-RF2500 development tools and MSP430FG4618/F2013 experimenter boards from Texas instruments," Master's thesis, Agri. and Mech. Col., Louisiana State Uni., Baton Rouge, LA, USA, 2011.

[25] W. Jindamaneepon, B. Rattanalert, K. Sengchuai, A. Booranawong, H. Saito, and N. Jindapetch, "A novel FPGA-based multi-channel multi-interface wireless node: Implementation and preliminary test," in *Proc. Adv. Comput. Commun. Eng. Technol.*, 2016, pp. 1163–1173.

[26] Y. Guo, K. Huang, N. Jiang, X. Guo, Y. Li, and G. Wang, "An exponential-Rayleigh model for RSS-based device-free localization and tracking," *IEEE Trans. Mobile Comput.*, vol. 14, no. 3, pp. 484–494, Mar. 2015.

[27] J. Wilson and N. Patwari, "Radio tomographic imaging with wireless networks," *IEEE Trans. Mobile Comput.*, vol. 9, no. 5, pp. 621–632, May 2010.

[28] A. Krause, C. Guestrin, A. Gupta, and J. Kleinberg, "Near-optimal sensor placements: Maximizing information while minimizing communication cost," in *Proc. 5th Int. Conf. Inf. Process. Sensor Netw.*, 2006, pp. 2–10.

[29] M. Younis and K. Akkaya, "Strategies and techniques for node placement in wireless sensor networks: A survey," *Ad Hoc Netw.*, vol. 6, no. 4, pp. 621–655, 2008.